Mechanism of Interlayer Transport on a Growing Au(111) Surface: 2D vs. 3D Growth

Abid Ali[a], Hannes Jónsson[a,b]

[a]*Science Institute and Faculty of Physical Sciences, University of Iceland, VR-III, 107 Reykjavík, Iceland*
[b]*Dept. of Chemistry, Brown University, Rhode Island 02912, USA*

Abstract

The atomic scale transitions corresponding to diffusion and interlayer transport of a Au adatom on the low energy, close packed Au(111) surface are studied using density functional theory calculations within the generalized gradient approximation. Minimum energy paths and estimates of activation energy are calculated for processes that influence whether the crystal grows layer-by-layer, i.e. 2D growth, or whether new islands tend to nucleate on top of existing islands resulting in 3D growth. Kinks on island edges turn out to provide paths for adatom descent with lower activation energy than straight steps. The energy barrier for an adatom to round the corner and enter a kink site is significantly higher. A descent mechanism that places an adatom near but not at a kink site can therefore promote the formation of a new row of step atoms and lead to the introduction of additional kink sites, thereby opening up new low activation energy paths for descent and promotion of 2D growth. The sites adjacent and above the step edge provide large binding energy for the adatom, especially at the B-type step, and form a trough along which the adatom can migrate before descending, thereby increasing the probability that an adatom finds a kink on the B-type step. These features of the energy landscape representing the interaction of a Au adatom with the surface point to the possibility of a re-entrant layer-by-layer growth mode of the low energy, close packed surface of the gold crystal.

1. Introduction

In some material growth applications the goal is to form nanoscale islands on a surface while in others the preferred growth mode is layer-by-layer. The morphology of the surface is typically governed by kinetic processes rather than thermodynamics because the surface temperature is kept low enough to prevent the mixing of components. An important consideration then is the rate of various atomic rearrangement processes, in particular those that lead to descent of adatoms from an upper layer to a lower layer, i.e. interlayer transport. Such

processes have been studied extensively for several metals, in particular platinum, but while gold is also an attractive metal in various applications, little work has been done so far on interlayer transport in gold crystal growth.

An energy barrier larger than the activation energy for diffusion on a flat surface typically exists for the descent of an adatom from an upper layer to a lower layer and it is referred to as the Ehrlich-Schwoebel (ES) barrier [1]. This can be most easily seen if an adatom sitting in a threefold site of an island on a (111) surface of an FCC crystal rolls over an island edge. Then one of the three bonds to the underlying atoms is broken to a larger extent than if the adatom is rolling over a bridge site in a diffusion hop on a flat surface. Several theoretical calculations [2, 3, 4] for transition metal surfaces have shown, however, that such descent processes occur by a concerted displacement mechanism rather than by a hop over the step edge. Nevertheless, a significant ES barrier is typically present. The identification of the relevant transition mechanisms and characterization of the energy landscape for adatom migration on a growing surface is essential for gaining an understanding of the atomic scale mechanism of crystal and thin film growth and the conditions that can promote either 2D or 3D growth.

Sometimes the ES barrier is estimated simply as the difference between the energy barrier for descent starting from a site adjacent to the step edge minus the activation energy for diffusion on the flat terrace. Theoretical calculations using empirical potential functions, such as the embedded atom method (EAM) [10, 11], that can be applied to large enough systems [3], as well as field ion microscope (FIM) measurements [5] surface show that the landscape is more complex. The site closest to the step edge can offer higher binding energy for the adatom, as can be understood from the low coordination of the step atoms (lower coordinated atoms form stronger bonds) but sites further away from the step can have lower binding energy than sites on the flat surface, leading to an excluded zone near the step edge, as has been observed in FIM measurements [6, 7, 8, 9]. The energy barrier for adatom hops along and above the step edge can be small, as has been seen in EAM [10, 11] calculations of Pt(111) [3], significantly smaller than either diffusion away from the step edge or descent to the lower layer. As a result, the adatom can be expected to diffuse along the top of the step edge. This increases the attempt frequency for descent but can also increase the probability of nucleation of a new island on top of an existing island.

It is important to use a single reference point when the energy of the adatom in various sites and at the transition state for atomic rearrangements is estimated. If the islands are large enough, the most likely landing site of an incoming atom is at a flat terrace and the majority species will be an adatom in the lowest energy site of an extended, flat terrace. The zero of energy is here taken to be the energy of an adatom at an FCC site of the Au(111) surface.

Measurements of growing metal surfaces, in particular (100) facet of copper, have shown that 2D growth can be achieved at surprisingly low temperature [12, 13]. When growth at higher temperature leads to three-dimensional growth, this phenomenon is referred to as re-entrant layer-by-layer growth [14]. It has

been documented particularly well for the growth of the (111) facet of platinum [14, 15, 16, 17]. It is not clear how common re-entrant layer-by-layer growth is, in particular whether it holds for Au(111), a metal that is commonly used in experimental studies of nanostructures.

The key challenge in gaining understanding of the way conditions affect the growth mode is to identify the relevant atomic scale transition mechanisms. Usually this is assumed and postulated based on intuition, but a robust method for finding minimum energy paths for transitions, such as the nudged elastic band (NEB) method [18, 19], makes the exploration of a large number of possible mechanisms feasible, as long as the computational effort in evaluating the system energy and atomic forces is not too large. Such calculations can reveal several unexpected mechanisms, as discussed below.

As an adatom migrates along the step edge, it is likely to run into defects such as kinks where a row of step atoms ends. It has been pointed out that kinks as well as corners of island edges (where A- and B-type steps meet) can affect the energy barrier for descent of a Pt adatom on the Pt(111) surface. This was first based on extensive exploration of transitions mechanisms using NEB and EAM potential function [3] and then later supported also by density functional theory (DFT) calculations [20]. There, it was shown that kink sites can offer significantly lower energy paths for descent as compared to straight edges. This is particularly important for B-type steps on Pt(111) since the activation energy for descent is estimated to be particularly large there [4] and the 3D islands formed in the intermediate temperature range tend to be triangular surrounded by B-type steps. An unexpected mechanism involving a concerted two atom displacement process where the adatom takes the place of an edge atom near – but not at – a kink site turned out to have a particularly low energy barrier. It is hard to verify such a mechanism experimentally for a one-component system since the atoms are indistinguishable. But, an experimental STM study of a Co adatom on a Pt(111) surface has indeed shown that a concerted displacement process facilitated by a kink site, is most likely to occur [21]. This could be inferred from the final state location of the Co atom.

In this article, we present studies of the energetics and transition mechanisms for a Au adatom on the Au(111) surface using NEB calculations where the energy of the system and atomic forces are evaluated using DFT within the generalized gradient approximation. In particular, we address the question whether kinks on steps play an important role in the interlayer transport and thereby the possibility that a Au(111) surface can show re-entrant layer-by-layer growth.

The article is organized as follows. The methods are described in section 2, including the systems studied, the electronic structure method used, and the method for finding minimum energy paths of transitions. Then, the results are presented in section 3 and a discussion presented in section 4. A brief conclusion is given in section 5.

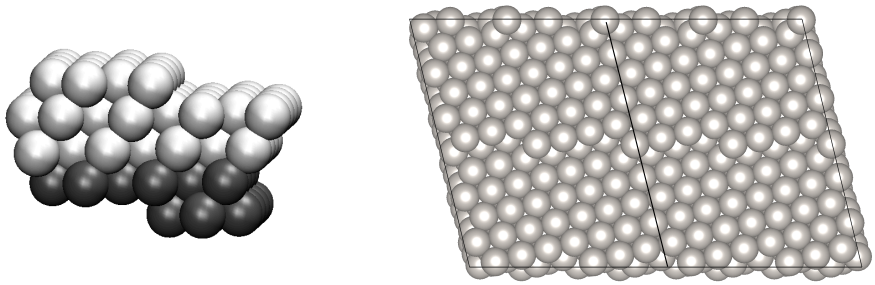

Figure 1: Left: Cross section of the slab with (221) surface Miller index, used to study the straight B-type step. Light gray spheres indicate atoms that can move freely, while dark gray spheres indicate atoms that are fixed in order to represent the confining effects of missing atoms below. Right: On-top view of two simulation cells used to represent kinks on the B-type step, with Miller index (985).

2. Methods

The flat Au(111) terrace is simulated using a slab of atomic layers containing 16 atoms subject to periodic boundary conditions in the plane of the surface. The atoms in the bottom two layers are kept fixed while atoms are free to move in the top layer. The binding energy of the adatom at an FCC site is used to define the zero of energy for the adatom in all the calculations presented here. It is important to have a single well defined zero of energy when such a complex energy landscape is explored. If the zero of energy is shifted to whatever happens to be the initial configuration of the transition studied, then an incorrect estimate is obtained for the activation energy.

The straight A-type step, which has a {100} microfacet, is represented by a slab with Miller index (322) while the straight B-type step, which has a {111} microfacet, is represented by a slab with index (221). These are periodic arrays of steps with short terraces in between. Such models have previously been used extensively in DFT studies of the properties of steps and atomic transitions, such as chemical reactions, at steps. Kinks on an A-type step are represented by a slab with Miller index (956) while kinks on a B-type step are represented by a slab with Miller index (985). These models are analogous to the (854) and (874) surface slabs used by Feibelman [22] in calculations of adatom diffusion along step bottoms, except that the width of the terraces in between the steps is larger in the (956) and (985) models, making them a more accurate representations of an island edge. These configurations contain between 150 and 200 atoms, a relatively large number making these systemds computationally demanding in electronic structure calculations. A cross section of the model used here to study a periodic B-type step and the model used to study kinks on the B-type step are shown in figure 1.

The electronic structure calculations are carried out using DFT [23, 24] within the generalized gradient approximation which is a step up in accuracy

from the local density approximation (LDA) [25]. The calculations are carried out with the PBEsol functional [26] as it gives good estimate of surface energy and lattice constant of solids, quantities that affect the strength of adatom interaction with the surface. The energy of a Au atom in the gas phase is likely to be overestimated by the PBEsol functional and the absolute value of the binding energy therefore overestimated (more towards LDA than functionals optimized for atoms and molecular bonding). But this is not of concern since the question addressed here is the variation of the energy of the adatom as it undergoes transitions on the solid surface, not the energy of the adatom with respect to a gas phase atom. The DFT/PBEsol calculations give a lattice parameter of 4.08 Å for Au crystal, in close agreement with the experimental value of 4.07 Å. The valence electrons are described using a plane wave basis while the effect of inner electrons is described using the projected augmented wave (PAW) formalism [27]. An energy cutoff of 300 eV is used in the plane wave expansion. A 2x2x1 k-point sampling is used with Methfessel-Paxton smearing [28] at a temperature of 0.1 eV. The reported energy values correspond to extrapolation to zero temperature. The VASP software is used in these calculations [29].

The minimum energy paths for the various transitions are calculated using the NEB method [18, 19] with the climbing image extension [30] and improved tangent estimate [31]. The initial paths are generated with the image dependent pair potential (IDPP) method [32]. The tolerance in the magnitude of atomic forces in optimizations of the atomic coordinates, both for identification of local minima and the images along the minimum energy paths, is 0.02 eV/Å. Typically, 5 intermediate images are used to represent paths in between the fixed endpoints, but this is specified further in the graphs below illustrating the calculated results.

Within the harmonic approximation to transition state theory (HTST), see review in ref. [20], the activation energy in the Arrhenius expression for the rate constant of an elementary transition is given by the highest energy along the minimum energy path, a first order saddle point on the energy surface, minus the energy of the initial state minimum. The activation energy for a given downstepping mechanism reported below is calculated as the difference in the saddle point energy and the energy of the adatom in a FCC site on the flat surface. The HTST rate theory is the standard approach in calculations of rates of crystal growth transitions. The pre-exponential factor in the Arrhenius expression can also be found by calculating the vibrational modes at the saddle point and in the initial state, but we will assume here that the value of the pre-exponential factor does not vary between mechanisms enough to make a significant difference in the rates and we compare only the values of the activation energy.

3. Results

The results of the NEB calculations of minimum energy paths are presented first for descent at steps, both straight and with a kink, and then paths for moving around a corner atom at a kink.

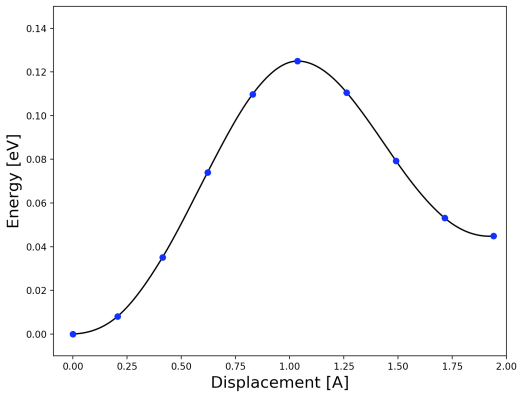

Figure 2: Energy along the minimum energy path for adatom hop from an FCC site to an HCP site on the flat Au(111) surface. The complete diffusion path involves analogous hop in reverse from the HCP site to another FCC site. The activation energy for diffusion is found to be 0.12 eV and the energy difference between the two sites is 0.04 eV. The energy of the adatom at the FCC site on the (111) surface is taken to be the zero of energy in all the results presented here.

Figure 2 shows the results obtained for a Au adatom diffusion hop on the flat (111) surface. The adatom starts at an FCC site and hops over a bridge to an HCP site where the binding energy is smaller by 0.04 eV. The completion of a diffusion path involves a second hop from the HCP site to another FCC site which is the reverse of the path shown. The activation energy for diffusion is found to be 0.12 eV. This is comparable to an estimate obtained in previous DFT calculations using the PBE functional, 0.15 eV (calculations using the more approximate LDA functional give 0.20 eV) [33].

3.1. Adatom descent

Figures 3 and 4 show calculated minimum energy paths for the descent of an adatom at A- and B-type steps with and without a kink. The initial site of the adatom is adjacent to the step edge, an HCP site in the case of the A-type step but an FCC site in the case of the B-type step. The binding energy at the HCP site adjacent to the A-type step is nearly equal to that of the FCC site of the flat Au(111) surface. The fact that the step atoms are undercoordinated and thereby form stronger bonds to the adatom compensates here the reduced binding energy at HCP sites as compared to FCC sites. At the B-type step edge, however, the adjacent site is of FCC type and the undercoordination of the step atoms leads to larger binding energy by 0.03 eV, as can be seen from the downward shift in the corresponding initial point of the descent path in figure 2. The activation energy is the energy of the maximum along the minimum energy path with respect to the adatom at the FCC site on a flat Au(111) surface. The calculated activation energy for three different descent paths at the two types of steps are summarized in Table 1.

The lowest activation energy for interlayer transport turns out to correspond to descent near a kink site on the B-type step. The initial site for this process is even lower in energy than the sites at the straight B-step, by about 0.1 eV and the activation energy for descent is 0.14 eV. This is substantially lower than the barrier for descent at a straight B-type step which is calculated to be 0.31 eV. Note that the final state energy is 0.3 eV higher for the path with lower activation energy because the final state does not correspond to an atom being placed at the 6-fold coordinated kink site but rather in a 5-fold coordinated site at the step edge. This shows that the height of the energy barriers does not scale with the final state energy. Such an approximation is, however, often invoked in crystal growth and chemical reaction calculations where energy barriers are not calculated but only estimated roughly.

The descent mechanism that involves placing an atom into the kink site at the B-type step rather than at the step edge near the kink site, corresponds to an intermediate value of the activation energy, 0.20 eV. The comparison of the two downstepping mechanisms at a kink on the B-type step again show that the activation energy does not scale with the energy of the final state.

Also for the A-type step, the kink offers paths for descent with lower activation energy than a straight step, but here the two kink related paths, the one that places an atom into the kink site and the one placing an atom at the step edge near the kink site, have similar activation energy, 0.16 and 0.17 eV. The lowest energy path for descent is, therefore, calculated to be descent near a kink site on the B-type step.

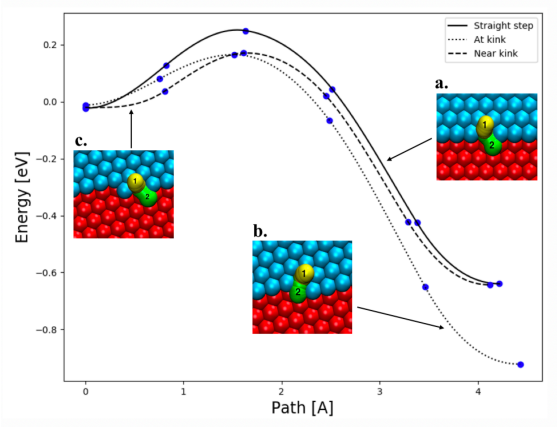

Figure 3: Energy along minimum energy paths for the descent of an adatom at a straight A-type step (solid line), at kink (dotted line) and near kink (dashed line). Insets show the configurations of the atoms in the nudged elastic band images of the minimum energy paths. Points on the curves show energy of the intermediate system images in the discretization of the paths. The atom that starts as an adatom at the upper terrace is labeled 1, while the step atom that gets pushed out is labeled 2. A kink site provides paths for adatom descent with lower activation energy than a straight step (see table 1 for numerical values).

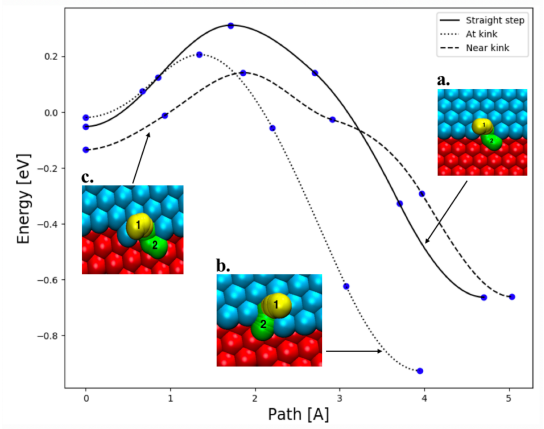

Figure 4: Energy along minimum energy paths for the descent of an adatom at a straight B-type step (solid line), at kink (dotted line) and near kink (dashed line). Insets show the configurations of the atoms in the nudged elastic band images of the minimum energy paths. Points on the energy curve show energy of the intermediate system images in the discretization of the paths. The atom that starts as an adatom at the upper terrace is labeled 1, while the step atom that gets pushed out is labeled 2. Remarkably, the lowest activation energy is obtained for a descent mechanism that places an atom at the step edge near a kink site but not in the kink site, even though this mechanism leads to significantly higher final state energy (see table 1 for numerical values).

Table 1: Results of DFT/PBEsol calculations of the activation energy for a Au adatom descent at A- and B-type steps on the Au(111) surface, with and without a kink. The activation energy is the highest energy along the minimum energy path minus the energy of an adatom in an FCC site on the Au(111) surface. The uncertainty in the difference between values of the activation energy for different transition mechanisms of this type has been estimated to be ca. 0.02 eV [4].

Step type	Mechanism	Activation energy
A		
	straight	0.25
	at kink	0.16
	near kink	0.17
B		
	straight	0.31
	at kink	0.20
	near kink	0.14

3.2. Rounding a corner

The preference for adatom descent into a site near but not at a kink site is important because it provides a seed for the formation of a new row of atoms and additional kink sites. A key issue then is whether such an atom can easily move from this rather high energy site to the nearby low energy kink site, either by rounding the corner atom or by a concerted displacement mechanism. The former mechanism turns out to have lower activation energy and the minimum energy paths for such transitions at both A-type and B-type steps are shown in figure 5. The insets show the atom configurations at the two endpoints and at each image in the converged NEB calculation of the transition path. The calculated energy barrier is large for both steps, over 0.5 eV, and the concerted displacement mechanism even higher, 0.7 eV. This means that an atom placed at a step after descent near a kink is not likely to move into the kink site if the temperature is not too high, for example at room temperature. The adatom can diffuse more readily along the step edge, with activation energy of 0.3 eV. This means that a new row of step atoms will form, introducing more kink sites and the low energy descent paths will, thereby, proliferate.

4. Discussion

The calculations presented here indicate that a Au adatom on top of an island on a Au(111) surface can descend to the lower layer most easily near a

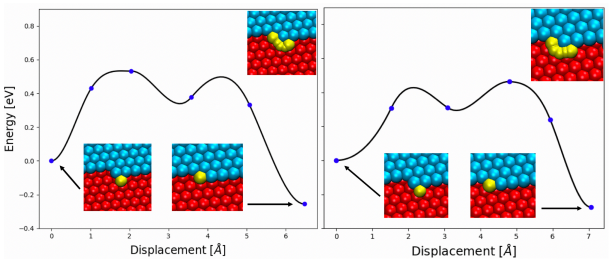

Figure 5: Energy along minimum energy paths for an adatom to move from a 5-fold coordinated site at a step edge into a nearby 6-fold coordinated kink site. Left: at A-type step. Right: at B-type step. Insets show the configurations of the atoms at the two endpoints and for images of the system in converged nudged elastic band calculations of the minimum energy paths. The activation energy is high in both cases, over 0.5 eV, significantly higher than for adatom descent. At a temperature where descent near a kink is active while the rounding of the corner to enter the kink site is not, the step edge becomes rough and the number of kink sites proliferates promoting layer-by-layer growth.

kink on a B-type step. This is similar to what has previously been deduced from calculations of a Pt adatom on a Pt(111) surface [3, 20]. This nonintuitive mechanism was first predicted from extensive studies of various mechanisms using an EAM potential function for the Pt/Pt(111) system [3]. It has been used to explain signs of re-entrant layer-by-layer growth in kinetic Monte Carlo simulations of Pt(111) surface growth [34]. Since the same feature in the energy landscape is found here for a Au adatom on a stepped gold surface, the indication is that Au(111) may also show re-entrant layer-by-layer growth behavior. The sites adjacent to and above the B-type step offer 0.03 eV stronger binding than corresponding sites on the A-type step, so adatoms will tend to migrate to the top of B-type step edges. As the energy barrier for rounding the corner into a kink site is more than three times larger than the energy barrier for descent, there will be a range in temperature where descent is active but rounding the corner is not, so the step edge will become rough with multiple kinks, each offering a low energy path for descent, and thereby promoting layer-by-layer growth.

Experimental STM measurements of Pt(111) growth have shown that the transition from 3D to 2D growth as temperature is lowered down to room temperature coincides with a transition from compact islands with relatively straight steps to dendritic islands with high density of kinks [17]. Straight step edges lead to significant activation energy for descent, especially B-type steps [4], while the presence of kinks offers low energy paths for descent that can be active even at low temperature. Thus, even though the thermal energy of the adatoms is reduced as the temperature is lowered, the number of low barrier paths for descent is increased enough by the increase in kink density so that 2D growth reappears as the temperature is lowered.

While the differences in activation energy between competing transition mechanisms calculated are small, on the order of 0.1 eV, which is often quoted

as an error bar for DFT calculations, the fact that only similar configurations of the system are being compared here and cancellation of errors can therefore be expected to be effective. The calculated activation energy differences presented here are likely meaningful and provide correct trends, for example in the comparison the different descent mechanisms. Also, the fact that various empirical potentials [3, 34] and STM experiments on a related system [21] show similar features indicates that kink sites do indeed offer low energy paths for adatom descent.

The results presented here demonstrate the complexity of the energy landscape and the importance of choosing a single reference point for the energy of the adatom. If the activation energy of a downstepping event is estimated as the increase in energy with respect to the energy of the initial state for the elementary event, then the comparison between A- and B-type steps will be incorrect. The initial state for the downstepping event is higher in energy at the A-type step than at the B-type step because it corresponds to an HCP site rather than an FCC site. The initial site for the descent near a kink on the B-type step is even lower in energy, as can be seen in figure 4. The proper energy reference for all the adatom descent mechanisms is the energy of the adatom in an FCC site of a flat terrace since this represents the majority species.

The results of the NEB-DFT/PBEsol calculations presented here illustrate that a number of processes need to be taken into account to determine the fate of an adatom that lands on top of an island, and thereby answer the question whether the atom deposition leads to 2D or 3D growth. Some of these features are subtle and unexpected, but they can control the surface morphology of a growing crystal. The challenge to theoretical studies is to identify the relevant processes and estimate the rate of these processes accurately enough to be able to explain the surface patterns observed in experimental measurements and to predict the growth mode of materials that have not been studied experimentally. The most serious challenge is the problem of identifying the relevant atomic scale processes. As the calculations presented here illustrate, the key process may be nonintuitive. This calls for efficient algorithms for finding which processes can occur in the system under study at given conditions.

Since classical dynamics simulations cannot cover long enough time scales, advanced techniques are needed to search for likely transition mechanisms [20, 35]. Long time scale simulation methods such as adaptive kinetic Monte Carlo [36, 37] have been used in combination with empirical potential functions in such studies, for example in simulations of Al(100) and Cu(100) growth [38], but the problem is that the more accurate and reliable DFT calculations have so far been computationally too demanding for such simulations. A possible future direction in this respect is the use of machine learning to interpolate between points in a training set of DFT calculations. The question still remains whether such an approach can be trusted to provide unexpected results since it represents only an interpolation between data fed into the machine learning algorithm. The most relevant part of the energy surface, corresponding to nonintuitive and unexpected mechanisms may be incorrectly represented since the training set will likely not contain such configurations. The challenge of explaining how

microscopic processes influence macroscopic behavior is particularly relevant in studies of growth shapes of crystals, which offer a unique testing ground for the computational challenges of bridging vast length and time scales.

As mentioned in the introduction, there is great interest in Au nanoparticles and therefore also the growth modes of Au nanoparticles. Recently, intriguing experimental observations have been made where Au nanoparticles were grown by reduction of precursors using an electron beam [39]. As a function of time, switches between disordered and ordered structures were observed until, eventually, as the nanoparticles became large enough the ordered structure dominated. More often, nanoparticles are grown by precipitation from solution, and there again it is important to gain an understanding of how the growth mode depends on conditions such as temperature and concentration of precursors [40]. Chemical vapor deposition can also be used, even one-step catalyst-free thermal chemical vapor deposition, as has been demonstrated in growth of Au nanoparticles on silicon substrates [41]. There, single-crystal nanoparticles with various morphologies such as prism, icosahedron, and five-fold twinned decahedron were formed. The shape of such nanoparticles is governed by the kinetic processes that take place as atoms land on the particle surface, including the processes studied here, as well as many others. A full description of the growth of nanoparticles requires calculations of additional atomic scale rearrangements, and then a long timescale simulations of the growth under specific conditions.

5. Conclusion

The theoretical results presented here, based on calculations of minimum energy paths for the descent of a Au adatom from atop an island into the growing layer, show that kinks on the step edge provide paths with lower activation energy than straight steps. This is found to be the case for both A- and B-type steps, as summarized in table 1. The binding energy of an adatom is particularly large at sites adjacent to and above the B-type step, so adatoms landing on top of an island are more likely to drift to such sites. At the straight B-type step, the activation energy for descent is found to be higher than at the A-type step, 0.31 eV *vs.* 0.25 eV, but a non-intuitive downstepping process that places an adatom next to – but not into – a kink site has a particularly low activation energy of 0.14 eV, representing essentially zero Ehrlich-Schwöbel barrier (the activation energy for diffusion on the flat (111) terrace is calculated to be 0.12 eV). This unexpected result illustrates that the activation for the various downstepping mechanisms does not scale with the final state energy, since a lower barrier leads to a higher energy final state in this case. The energy barrier for an adatom at the bottom of a step edge to round the corner and enter a kink site is found to be large, so the non-intuitive downstepping near a kink on a B-type step will likely lead to the formation of a new row of step atoms and thereby more kink sites, offering larger number of low barrier paths for descent.

The features of the energy landscape representing the interaction of a Au adatom with the crystal surface described above are in many ways similar to those found earlier for a Pt adatom on a Pt(111) surface and one can expect

similar growth modes to occur. While layer-by-layer growth is in any case going to be taking place at a temperature that is high enough for the adatoms to overcome energy barriers for downstepping, an intermediate temperature range where diffusion along island edges is active and the steps therefore tend to be straight and free of kinks will likely give 3D growth since the barrier for descent at straight steps is relatively high, significantly higher than diffusion on the flat terrace. The corresponding Ehrlich-Schwöbel barrier is 0.2 eV at the B-type step. Then, as the temperature is lowered further and diffusion of adatoms along the step bottoms becomes hindered, the steps will develop kinks and a new low barrier descent mechanism becomes available. Since the downstepping at kinks on a B-type step is most likely going to place an adatom near but not at a kink site, a new row of step atoms is nucleated, generating new kinks and additional low barrier paths for descent. This can lead to re-entrant layer-by-layer growth, as has been observed experimentally for Pt(111). The main conclusion of the work presented here is, therefore, that Au(111) growth is likely to show re-entrant layer-by-layer behavior analogous to that of Pt(111). This can have significant consequences for the various methods that are being developed for growing Au nanoparticles of particular shape. The functionality of Au nanoparticles in various applications, such as catalysis, is strongly dependent on the shape of the nanoparticle and thereby the abundance of the various types of sites on the surface.

6. Acknowledgement

This work was funded by the European Union's Horizon 2020 research and innovation programme under the Marie Sklodowska Curie Innovative Training Network ELENA, grant agreement No. 722149 and by the Icelandic Science Fund.

[1] R. L. Schwöbel and E. J. Shipsey, 'Step motion on crystal surfaces', *J. Appl. Phys.* **37**, 3682 (1966); G. Ehrlich and F. G. Hudda, 'Atomic view of surface self-diffusion: Tungsten on tungsten', *J. Chem. Phys.* **44**, 1039 (1966).

[2] M. Villarba and H. Jónsson, 'Low temperature homoepitaxial growth of Pt(111) in simulated vapor deposition', *Phys. Rev. B* **49**, 2208 (1994).

[3] M. Villarba and H. Jónsson, 'Diffusion mechanisms relevant to metal crystal growth: Pt/Pt(111)', *Surf. Sci.* **317**, 15 (1994).

[4] P. J. Feibelman, 'Interlayer self-diffusion on stepped Pt(111)', *Phys. Rev. Lett.* **81**, 168 (1998).

[5] S. C. Wang and G. Ehrlich, 'Atom incorporation at surface clusters: An atomic view', *Phys. Rev. Lett.* **67**, 2509 (1991).

[6] S. C. Wang and G. Ehrlich, 'Adatom motion to lattice steps: A direct view', *Phys. Rev. Lett.* **70**, 41 (1993).

[7] S. C. Wang and G. Ehrlich, 'Atom condensation at lattice steps and clusters', *Phys. Rev. Lett.* **71**, 4174 (1993).

[8] A. Gölzhäser and G. Ehrlich, 'Atom movement and binding on surface clusters: Pt on Pt(111) clusters', *Phys. Rev. Lett.* **77**, 1334 (1996).

[9] K. Kyuno and G. Ehrlich, 'Step-edge barriers: An atomistic view', *Phys. Rev. Lett.* **81**, 5592 (1998).

[10] M. S. Daw and M. I. Baskes, 'Embedded-atom method: Derivation and application to impurities, surfaces, and other defects in metals', *Phys Rev. B* **29**, 6443 (1984).

[11] M.S. Daw, 'Model of metallic cohesion: The embedded-atom method', *Phys. Rev. B* **39**, 7441 (1989).

[12] J. J. de Miguel, A. Sanchez, A. Cebollada, J. M. Callego, J. Ferron, and S. Ferrer, 'The surface morphology of a growing crystal studied by thermal energy atom scattering (TEAS)', *Surf. Sci.* **189/190**, 1062 (1987).

[13] W.F. Egelhoff and I. Jacob, 'Reflection High-Energy Electron Diffraction (RHEED) Oscillations at 77 K', *Phys. Rev. Letters* **62**, 921 (1989).

[14] R. Kunkel, B. Poelsema, L. K. Verheij, and G. Comsa, 'Reentrant layer-by-layer growth during molecular-beam epitaxy of metal-on-metal substrates', *Phys. Rev. Letters* **65**, 733 (1990).

[15] B. Poelsema, R. Kunkel, N. Nagel, A. F. Becker, G. Rosenfeld, L. K. Verheij, and G. Comsa, 'New phenomena in homoepitaxial growth of metals'; *Appl. Phys.* **A 53**, 369 (1991).

[16] B. Poelsema, A. Becker, G. Rosenfeld, R. Kunkel, N. Nagel, L. K. Verheij, and G. Comsa, 'On the shape of the in-phase TEAS oscillations during epitaxial growth of Pt(111) *Surf. Sci.* **272**, 269 (1992).

[17] M. Kalf, G. Comsa, and T. Michely, 'How sensitive is epitaxial growth to adsorbates', *Phys. Rev. Lett.* **81**, 1255 (1998).

[18] G. Mills, H. Jónsson and G. K. Schenter, 'Reversible work transition state theory: application to dissociative adsorption of hydrogen', *Surf. Sci.* **324**, 305 (1995).

[19] H. Jónsson, G. Mills, and K. W. Jacobsen, in *Classical and Quantum Dynamics in Condensed Phase Simulations*, ed. B. J. Berne, G. Ciccotti, and D. F. Coker, page 385 (World Scientific, 1998).

[20] H. Jónsson, 'Theoretical studies of atomic scale processes relevant to crystal growth', *Annual Review of Physical Chemistry* **51**, 623 (2000).

[21] E. Lundgren, B. Stanka, G. Leonardelli, M. Schmid and P. Varga, 'Interlayer diffusion of adatoms: A scanning-tunneling microscopy Study', *Phys. Rev. Lett.* **82**, 5068 (1999).

[22] P. J. Feibelman, 'Self-diffusion along step bottoms on Pt(111)', *Phys. Rev. B* **60**, 4972 (1999).

[23] P. Hohenberg and W. Kohn, 'Inhomogeneous electron gas', *Phys. Rev.* **136**, B864 (1964)

[24] W. Kohn and L. J. Sham, 'Self-consistent equations including exchange and correlation effects', *Phys. Rev.* **140**, A1133 (1965).

[25] J. P. Perdew, 'Jacob's ladder of density functional approximations for the exchange-correlation energy', *AIP Conference Proceedings* **577**, 1 (2001).

[26] J. P. Perdew, J. P. Perdew, A. Ruzsinszky, G. I. Csonka, O. A. Vydrov, G. E. Scuseria, L. A. Constantin, X. Zhou and K. Burke, 'Restoring the density-gradient expansion for exchange in solids and surfaces', *Phys. Rev. Lett.* **100**, 136406 (2008); *Phys. Rev. Lett.* **102**, 039902 (2009).

[27] P. E. Bloechl, 'Projector augmented-wave method', *Phys. Rev. B* **50**, 17953 (1994).

[28] M. Methfessel and A.T. Paxton, 'High-precision sampling for Brillouin-zone integration in metals', *Phys. Rev. B* **40**, 3616 (1989).

[29] G. Kresse and J. Hafner, *Phys. Rev. B* **47**, 558 (1993); **49**, 14251 (1994); G. Kresse and J. Furthmüller, *Comput. Mater. Sci.* **6**, 16 (1996); *Phys. Rev. B* **55**, 11169 (1996).

[30] G. Henkelman, B. Uberuaga and H. Jónsson, 'A Climbing-Image NEB Method for Finding Saddle Points and Minimum Energy Paths' *J. Chem. Phys.* **113**, 9901 (2000).

[31] G. Henkelman and H. Jónsson, 'Improved Tangent Estimate in the NEB Method for Finding Minimum Energy Paths and Saddle Points', *J. Chem. Phys.* **113**, 9978 (2000).

[32] S. Smidstrup, A. Pedersen, K. Stokbro and H. Jónsson, 'Improved initial guess for minimum energy path calculations', *J. Chem. Phys.* **140**, 214106 (2014).

[33] JJ. Mortensen, Bj. Hammer, Bjørk and Nielsen, Ole Holm and KW. Jacobsen and JK. Nørskov 'Density functional theory study of self-diffusion on the (111) surfaces of Ni, Pd, Pt, Cu, Ag and Au' *Springer Series on Solid State Physics* **121**, 173 (1996).

[34] J. Jacobsen, K. W. Jacobsen, P. Stoltze, and J. K. Nørskov, 'Island shape-induced transition from 2D to 3D growth for Pt/Pt(111)', *Phys. Rev. Lett.* **74**, 2295 (1995).

[35] H. Jónsson, 'Simulation of surface processes', *Proceedings of the National Academy of Sciences* **108**, 944 (2011).

[36] G. Henkelman and H. Jónsson, 'Long time scale kinetic Monte Carlo simulations without lattice approximation and predefined event table', *J. Chem. Phys.* **115**, 9657 (2001).

[37] S.T. Chill, M. Welborn, R. Terrell, L. Zhang, J-C. Berthet, A. Pedersen, H. Jónsson and G. Henkelman, 'EON: Software for long time simulations of atomic scale systems', *Modelling and Simulation in Materials Science and Engineering* **22**, 055002 (2014).

[38] G. Henkelman and H. Jónsson, 'Multiple time scale simulations of metal crystal growth reveal importance of multi-atom surface processes', *Phys. Rev. Letters* **90**, 116101 (2003).

[39] S. Jeon *et al.* 'Reversible disorder-order transitions in atomic crystal nucleation', *Science* **371**, 498 (2021).

[40] T. Nguyen, K. Thanh, N. Maclean and S. Mahiddine, 'Mechanisms of Nucleation and Growth of Nanoparticles in Solution', *Chem. Rev.* **114**, 7610 (2014).

[41] S. Manna, J. Woo Kim, Y. Takahashi, O. G. Shpyrko and E. E. Fullerton, 'Synthesis of single-crystalline anisotropic gold nano-crystals via chemical vapor deposition', *Journal of Applied Physics* **119**, 174301 (2016).